*Journal of Engineering Mathematics* **24**: 1–23, 1990.



# Study of the axially symmetric motion of an incompressible viscous fluid between two concentric rotating spheres

J.C. GAGLIARDI,[1] N.J. NIGRO,[2,*] A.F. ELKOUH,[2] J.-K. YANG,[2] and L. RODRIGUEZ, SJ[2]

[1]*Bureau of Mines Research Division, Fort Snelling, Minnesota, USA*
[2]*Department of Mechanical Engineering, Marquette University, Milwaukee, Wisconsin 53233, USA* (*author for correspondence)

Received 18 September 1987; accepted in revised form 20 March 1989

**Abstract.** The research reported herein involves the study of the steady state and transient motion of a system consisting of an incompressible, Newtonian fluid in an annulus between two concentric, rotating, rigid spheres. The primary purpose of the research is to study the use of an approximate analytical method for analyzing the transient motion of the fluid in the annulus and the spheres which are started suddenly due to the action of prescribed torques. The problems include cases where: (a) one (or both) spheres rotate with prescribed constant angular velocities and (b) one sphere rotates due to the action of an applied constant or impulsive torque.

In this research, the coupled solid and fluid equations of motion are linearized by employing the perturbation technique. The meridional dependence in these equations is removed by expanding the dependent variables in a series of Gegenbauer functions with variable coefficients and employing the orthogonality property of these functions. The equations for the variable coefficients are solved by separation of variables and Laplace transform methods. Results for the stream function, circumferential function, angular velocity of the spheres and torque coefficient are presented as a function of time for various values of the dimensionless system parameters.

## 1. Introduction

The problem involving the steady-state motion of a viscous, incompressible fluid contained in an annulus between two concentric spheres which rotate about a common axis with an angular velocity which has been prescribed a priori has been the subject of extensive research in engineering, meteorology and geophysics. Proudman [1], Stewartson [2], Carrier [3], Haberman [4], and Munson and Joseph [5] obtained an approximate analytical solution to the problem involving the flow in an annulus between two spheres rotating with prescribed constant angular velocities. Pedlosky [6] extended the problem to include temperature effects. Dennis and Singh [7] solved this problem by employing a quasi-analytical method; i.e., they expanded the stream function, vorticity, and the circumferential function in a series of orthogonal functions and then solved the resulting system of ordinary differential equations numerically. Greenspan [8], Schultz and Greenspan [9], Schrauf [10], and Bar-Yoseph, Blech and Solan [11] solved this problem by employing numerical methods.

Experimental results have been obtained for the steady-state problem by a number of investigators. Sorokin, Khlebutin, and Shaidurov [12], Khlebutin [13], Sawatzki and Zierep [14], Munson and Menguturk [15], Wimmer [16, 17], Nakabayashi [18] and Waked and Munson [19, 20] studied the problem involving flow in an annulus between two spheres where either the inner or the outer sphere rotates with constant angular velocity. Munson and Douglass [21] obtained experimental (and theoretical) results for the problem where the inner sphere is subjected to a prescribed oscillatory (sinusoidal) motion.

The problem involving the transient motion of a fluid contained in an annulus between two concentric rotating spheres has received less attention in the literature. Pearson [22, 23], Dennis and Quartapelle [24], Krause and Bartels [25], and Bartels [26] employed the finite-difference method to obtain a solution to the transient problem for the case where one of the spheres is suddenly rotated and then held at a prescribed constant angular velocity. The study of this problem for a sphere rotating in an infinite medium has been conducted by Illingworth [27], Benton [28], Barrett [29], Dennis and Ingham [30], Dennis, Singh, and Ingham [31], and Takagi [32]. To date, there has been no published research involving the transient motion of a viscous fluid contained in an annulus between rotating spheres where the angular velocities of the spheres are not prescribed a priori; i.e., where the motion of the system is a result of the coupling (interaction) between the fluid and the spheres. Recently, Yang [33] studied this problem by employing the finite-difference method.

The primary purpose of this research is to study the use of an approximate analytical method for analyzing the transient flow of a viscous incompressible fluid contained in an annulus between two spheres which are started suddenly due to the action of prescribed torques, instead of prescribed angular velocities. With this method, the equations of motion for the rigid body and the fluid are expressed in terms of a stream function ($\Psi$) and a circumferential function ($\Omega$), and then linearized for small values of Reynolds number by use of the perturbation method. The dependence of $\Psi$ and $\Omega$ on the meridional coordinate $\theta$ is removed by expanding the dependent variables in a series of Gegenbauer functions with variable coefficients and employing the orthogonality property of these functions. This approach was utilized successfully for the steady-state problem by Munson and Joseph [5] who employed Legendre polynomials instead of Gegenbauer functions. However, Dennis and Singh [7] found the Gegenbauer functions to be more appropriate for this problem. The resulting equations for the variable coefficients are then solved by employing the Laplace transform method (to obtain the zeroth-order approximation) and the separation of variables method (to obtain the higher-order approximations). Results for $\Psi$, $\Omega$, angular velocities of the spheres, torque coefficients, and fluid angular momentum are presented as a function of various values of the dimensionless system parameters.

## 2. Mathematical model

The system under study consists of an isothermal, incompressible, Newtonian fluid contained in an annulus between two concentric rotating rigid spheres (see Fig. 1). The inner and outer radius of the annulus are $r_1^*$ and $r_2^*$, respectively. The spheres are assumed to be rigid, and constrained to rotate about the $z^*$ axis under the action of externally applied torques.

The fluid velocity components in the direction of the spherical coordinates $r^*$, $\theta$, and $\phi$ are given as $u^*$, $v^*$, and $w^*$, respectively. The flow is independent of the coordinate $\phi$ due to axial symmetry about the spin axis. The transformation equations which relate the fluid velocity components to the stream function ($\Psi^*$) and circumferential function ($\Omega^*$) are given as

$$u^* = -\frac{1}{r^{*2}}\Psi^*_{,x}, \qquad v^* = -\frac{1}{r^*(1-x^2)^{1/2}}\Psi^*_{,r}, \qquad w^* = \frac{\Omega^*}{r^*(1-x^2)^{1/2}} \tag{1}$$

where

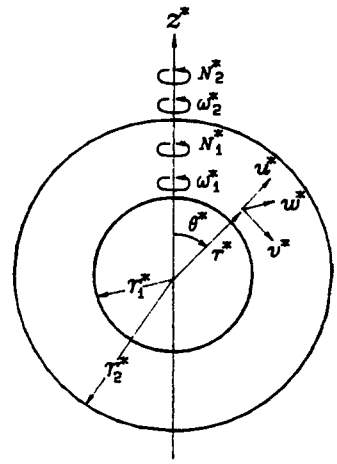


*Fig. 1.* Notation for flow in spherical annulus problem.

$$x = \cos\theta\,, \qquad \Psi^*_{,x} = \frac{\partial \Psi^*}{\partial x} \qquad \text{and} \qquad \Psi^*_{,r} = \frac{\partial \Psi^*}{\partial r^*}\,.$$

The form of (1) for $u^*$ and $v^*$ is such that the continuity equation is automatically satisfied. The system variables in this equation are expressed in dimensionless form by employing the following transformations:

$$r = \frac{r^*}{r_o^*}\,, \qquad t = \frac{t^* \nu^*}{r_o^{*2}}\,, \qquad \omega = \frac{\omega^*}{\omega_o^*}\,, \qquad \Psi = \frac{\Psi^*}{\omega_o^* r_o^{*3}}\,, \qquad \Omega = \frac{\Omega^*}{\omega_o^* r_o^{*2}}\,, \tag{2}$$

where

$\nu^*$ = kinematic viscosity,

$r_o^*$ = reference radius,

$\omega_o^*$ = reference angular velocity.

The equations of motion for the fluid are developed in vorticity form by taking the curl of the Navier–Stokes equations. This yields

$$\frac{1}{R} M(\Omega) = \frac{1}{r^2} [\Psi_{,r}\Omega_{,x} - \Psi_{,x}\Omega_{,r}]\,, \tag{3a}$$

$$\frac{1}{R} L(M\Psi) = \frac{2\Omega}{r^3}\left[\frac{rx}{(1-x^2)}\,\Omega_{,r} + \Omega_{,x}\right] + \frac{1}{r^2}[\Psi_{,r} L(\Psi_{,x}) - \Psi_{,x} L(\Psi_{,r})] + \frac{2L(\Psi)}{r^3}\left[\frac{rx}{(1-x^2)}\,\Psi_{,r} + \Psi_{,x}\right], \tag{3b}$$

where

$$L = \frac{\partial^2}{\partial r^2} + \frac{1}{r^2}(1-x^2)\frac{\partial^2}{\partial x^2}\,, \qquad M = \left(L - \frac{\partial}{\partial t}\right), \tag{4}$$

$$R = \text{Reynolds number} = \frac{\omega_o^* r_o^{*2}}{\nu^*} . \tag{5}$$

The equation of motion for the inner or outer sphere rotating under the action of an applied torque is

$$\left(\frac{1}{5}\right) I_q \omega_{q,t} + \frac{3}{2} \int_0^1 [r_q (r_q \Omega_{,r}[r_q, x, t] - 2\Omega[r_q, x, t])] \, dx = N_q , \tag{6a}$$

$$\omega_q(0) = 0 , \tag{6b}$$

where

$q = 1, 2$ (subscripts referring to inner and outer sphere, respectively),

$r_q = r_q^*/r_o^*$ ,

$r_q^*$ = inner or outer radius of the annulus,

$\omega_q = \omega_q^*/\omega_o^*$ ,

$\omega_q^*$ = angular velocity of the inner or outer sphere,

$$I_q = \left(\frac{15}{8\pi}\right) \frac{J_q^*}{\rho_f^* r_o^{*5}} ,$$

$J_q^*$ = mass moment of inertia of the inner or outer sphere,

$\rho_f^*$ = density of the fluid,

$$N_q = \left(\frac{3}{8\pi}\right) \frac{N_q^*}{\mu^* r_o^{*3} \omega_o^*} , \tag{7}$$

$N_q^*$ = external torque applied to the inner or outer sphere,

$\mu^* = \rho_f^* \nu^*$ .

The equations which result from the symmetry of the flow in the annulus are

$$\Omega[r, 1, t] = 0 , \qquad \Psi[r, 1, t] = 0 , \qquad L\Psi[r, 1, t] = 0 , \tag{8a,b,c}$$

$$\Omega_{,x}[r, 0, t] = 0 , \qquad \Psi[r, 0, t] = 0 , \qquad L\Psi[r, 0, t] = 0 . \tag{8d,e,f}$$

The conditions which must be satisfied at the interfaces of the fluid and solid are

$$\frac{\Omega[r_q, x, t]}{r_q^2(1 - x^2)} = \omega_q , \qquad \Psi[r_q, x, t] = 0 , \qquad \Psi_{,r}[r_q, x, t] = 0 , \quad \text{for } q = 1, 2 . \tag{9a,b,c}$$

In this analysis the fluid inside the spherical annulus is initially at rest; hence, the initial conditions for the fluid are

$$\Omega[r, x, 0] = \Psi[r, x, 0] = 0 . \tag{10}$$

The cases which are discussed in this paper consist of the following, or combinations of the following: (a) the inner (or outer) sphere is started from rest with a prescribed constant angular velocity (i.e., step-function input), and (b) the inner (or outer) sphere is started from rest due to the action of a prescribed impulsive torque. A third case in which the inner (or outer) sphere is started from rest due to the action of a prescribed constant torque is discussed in [34]. The reference angular velocity in case (a) is chosen to be the larger of the two prescribed angular velocities. Note that, for this case, (6a) and (6b) are not required since $\omega_q$ is prescribed. The reference angular velocity for case (b) is computed by applying the impulse-momentum principle.

The viscous torque ($T_q^*$) acting on the inner or outer sphere can be evaluated by integrating the shearing stress ($\tau_{\phi r}^*$) over the corresponding spherical surface. The expression for the torque is given in dimensionless form as

$$T_q = \frac{3}{2}\int_0^1 [r_q(r_q\Omega_{,r}[r_q, x, t] - 2\Omega[r_q, x, t])]\,\mathrm{d}x\,, \tag{11}$$

where

$$T_q = \left(\frac{3}{8\pi}\right)\frac{T_q^*}{\mu^*\omega_o^* r_o^{*3}}\,, \qquad q = 1, 2\,.$$

## 3. Analysis

### *3.1. Perturbation method*

The mathematical model was linearized for small values of $R_q$ by employing the perturbation method. For this purpose, the dependent variables are expressed as follows:

$$\Omega = \sum_{k=0}^{\infty}(R_q)^k\Omega^{(k)}\,, \qquad \Psi = \sum_{l=1}^{\infty}(R_q)^l\Psi^{(l)}\,, \tag{12a}$$

$$N_q = \sum_{k=0}^{\infty}(R_q)^k N_q^{(k)}\,, \qquad \omega_q = \sum_{k=0}^{\infty}(R_q)^k\omega_q^{(k)}\,, \tag{12b}$$

$$T_q = \sum_{k=0}^{\infty}(R_q)^{(k)}T_q^{(k)}\,, \tag{12c}$$

where $k = 0, 2, 4, \ldots$, $l = 1, 3, 5, \ldots$ and

$R_q$ = Reynolds number based on $r_o^* = r_q^*(q = 1, 2)$.

Substituting (12a) and (12b) into (3a), (3b) and equating coefficients of like powers of $R_q$ yields

$$M(\Omega^{(k)}) = \frac{1}{r^2}\sum_{m=0}^{k-2}[\Psi_{,r}^{(k-m-1)}\Omega_{,x}^{(m)} - \Psi_{,x}^{(k-m-1)}\Omega_{,r}^{(m)}]\,, \tag{13a}$$

$$L(M\Psi^{(l)}) = \frac{2}{r^3}\sum_{m=0}^{l-1}\left[\Omega^{(l-m-1)}\left(\frac{rx\Omega^{(m)}_{,r}}{(1-x^2)} + \Omega^{(m)}_{,x}\right)\right]$$
$$+ \frac{1}{r^2}\sum_{n=1}^{l-2}\left[\Psi^{(l-n-1)}_{,r}\{L(\Psi^{(n)}_{,x})\} - \Psi^{(l-n-1)}_{,x}\{M(\Psi^{(n)}_{,r})\}\right]$$
$$+ \frac{2}{r^3}\sum_{n=1}^{l-2}\left[L\Psi^{(l-n-1)}\left(\frac{rx\Psi^{(n)}_{,r}}{(1-x^2)} + \Psi^{(n)}_{,x}\right)\right]. \tag{13b}$$

In a similar manner, for the impulsive torque problem, equation (6a) yields

$$\left(\frac{1}{5}\right)I_q\omega^{(k)}_{q,t} + \frac{3}{2}\int_{x=0}^{x=1}[r_q(r_q\Omega^{(k)}_{,r} - 2\Omega^{(k)}]\,dx = 0\,,$$
$$\omega_q(0) = \omega_{q0}\,, \tag{14}$$

where $k, m = 0, 2, 4, \ldots, k - m \geqslant 2$, $l, n = 1, 3, 5, \ldots, l - n \geqslant 2$, $q = 1, 2$, and

$\omega_{q0}$ = the equivalent initial angular velocity computed with the use of the impulse-momentum principle.

Finally, substitution of (12a) into (8), (9) and (10) yields

$$\Omega^{(k)}[r, 1, t] = \Psi^{(l)}[r, 1, t] = 0\,, \tag{15a}$$

$$L\Psi^{(l)}[r, 1, t] = \Omega^{(k)}_{,x}[r, 0, t] = 0\,, \tag{15b}$$

$$\Psi^{(l)}[r, 0, t] = L\Psi^{(l)}[r, 0, t] = 0\,, \tag{15c}$$

$$\frac{\Omega^{(k)}[r_q, x, t]}{r_q^2(1-x^2)} = \omega_q^{(k)}\delta_{k0}\,, \tag{16a}$$

$$\Psi^{(l)}[r_q, x, t] = 0\,, \qquad \Psi^{(l)}_{,r}[r_q, x, t] = 0\,, \tag{16b}$$

$$\Omega^{(k)}[r, x, 0] = \Psi^{(l)}[r, x, 0] = 0\,, \tag{17}$$

where $k = 0, 2, 4, 6, \ldots, l = 1, 3, 5, \ldots, q = 1, 2$, and

$\delta_{k0} = 1$ if $k = 0$,
$= 0$ if $k \neq 0$.

The expressions for the $k^{\text{th}}$ order approximations of the dimensionless viscous torque were obtained in the same manner by substituting (12c) into (11) and equating coefficients on like powers of $R_q$. This yields

$$T_q^{(k)} = \frac{3}{2}\int_0^1 [r_q(r_q\Omega^{(k)}_{,r}[r_q, x, t] - 2\Omega^{(k)}[r_q, x, t])]\,dx\,, \tag{18}$$

where $k = 0, 2, 4, \ldots$ and $q = 1, 2$.

*3.2. Form of equations governing* $\Psi^{(l)}$ *and* $\Omega^{(k)}$

The form of the solution for $\Psi^{(l)}$ and $\Omega^{(k)}$ was expanded in a series as follows:

$$\Omega^{(k)} = \sum_{i=0}^{k} I_{i+2}(x) f_i^{(k)}(r, t) , \tag{19a}$$

$$\Psi^{(l)} = \sum_{j=1}^{l} I_{j+2}(x) g_j^{(l)}(r, t) , \tag{19b}$$

where $i, k = 0, 2, 4, \ldots$; $j, l = 1, 3, 5, \ldots$, and

$I_n(x)$ = Gegenbauer polynomials.

The general form of the series given in (19) was employed by Munson and Joseph [5]; however, they expanded in terms of Legendre polynomials instead of Gegenbauer polynomials. The equations governing the functions $I_n(x)$ were obtained by employing the separation of variables method in conjunction with the equations $M(\Omega^{(k)}) - M(\Psi^{(l)}) = 0$. This yields

$$(1 - x^2) I_{n,xx}(x) + \alpha I_n(x) = 0 , \tag{20}$$

where $\alpha$ = separation constant, and if $\alpha = n(n-1)$, then

$I_n(x) = n^{\text{th}}$ order Gegenbauer function,

$$= \frac{-1}{(n-1)!} \left(\frac{\mathrm{d}}{\mathrm{d}x}\right)^{n-2} \left(\frac{x^2 - 1}{2}\right)^{n-1} , \quad \text{for } n = 2, 3, 4, \ldots . \tag{21}$$

The Gegenbauer polynomials generated from (21) automatically satisfy the required symmetry conditions given in (8). They also satisfy the following orthogonality condition:

$$\int_{-1}^{1} \frac{I_m(x) I_n(x)\, \mathrm{d}x}{(1 - x^2)} = \frac{2}{n(n-1)(2n-1)} , \quad m = n ,$$

$$= 0 , \qquad m \neq n . \tag{22}$$

The equations governing the variable coefficients $f_i^{(k)}$ and $g_j^{(l)}$ are obtained by: (a) substituting (19) into (13), (b) multiplying the resulting equations by $I_{p+2}/(1 - x^2)$, (c) integrating each term in the equations over the region $-1 \leqslant x \leqslant 1$ and (d) applying the orthogonality property defined in (22). This yields

$$f_{i,rr}^{(k)} - \left[\frac{(i+1)(i+2)}{r^2}\right] f_i^{(k)} - f_{i,t}^{(k)} = \frac{(i+1)(i+2)(2i+3)}{2} \left(\frac{1}{r^2}\right) \sum_{m=0}^{k-2} \Gamma_1^{(k,m)} , \tag{23a}$$

$$g^{(l)}_{j,rrrr} - \left[\frac{2(j+1)(j+2)}{r^2}\right] g^{(l)}_{j,rr} + \left[\frac{4}{r^3}(j+1)(j+2)\right] g^{(l)}_{j,r} + \left[\frac{(j+1)(j+1)}{r^4}[(j+1)(j+2)-6]\right] g^{(l)}_{j} - g^{(l)}_{j,rrt} + \left[\frac{(j+1)(j+2)}{r^2}\right] g^{(l)}_{j,t} = \frac{(j+1)(j+2)(2j+3)}{2}\left[\left(\frac{2}{r^3}\right)\sum_{m=0}^{l-1}\Gamma_2^{(l,m)} + \sum_{n=1}^{l-2}\left(\left(\frac{1}{r^2}\right)(\Gamma_3^{(l,n)} + \Gamma_4^{(l,n)}) + \left(\frac{2}{r^3}\right)\Gamma_5^{(l,n)}\right)\right], \tag{23b}$$

where

$$\Gamma_1^{(k,m)} = \sum_{jj=1}^{k-m-1}\sum_{it=0}^{m}[R(i, jj, ii)g^{(k-m-1)}_{jj,r} f^{(m)}_{it} - R(i, ii, jj)g^{(k-m-1)}_{jj} f^{(m)}_{it,r}], \tag{24a}$$

$$\Gamma_2^{(l,n)} = \sum_{ij=0}^{l-m-1}\sum_{it=0}^{m}[Q(j, ij, ii)rf^{(m)}_{i,r} + R(i, ij, ii)f^{(m)}_{it}]f^{(l-m-1)}_{ij}, \tag{24b}$$

$$\Gamma_3^{(l,m)} = \sum_{jj=1}^{l-m-1}\sum_{jt=1}^{m}\left[R(j, ji, jj)g^{(l-m-1)}_{jj,r}\left(g^{(m)}_{jt,rr} - \frac{(ji+1)(ji+2)}{r^2} g^{(m)}_{jt}\right)\right], \tag{24c}$$

$$\Gamma_4^{(l,m)} = \sum_{jj=1}^{l-m-1}\sum_{ji=1}^{m}\left[R(j, ji, jj)g^{(l-m-1)}_{jj}\left(g^{(m)}_{jt,rrr} - \frac{(ji+1)(ji+2)}{r^2} g^{(m)}_{ji,r}\right)\right], \tag{24d}$$

$$\Gamma_5^{(l,m)} = \sum_{jj=1}^{l-m-1}\sum_{ji=1}^{m}[Q(j, jj, ji)g^{(m)}_{i} + R(j, jj, ji)rg^{(m)}_{ji,r}] \times\left[g^{(l-m-1)}_{ji,rr} - \frac{(ji+1)(ji+2)}{r^2} g^{(l-m-1)}_{jt}\right], \tag{24e}$$

$$R(j, jj, ji) = \int_{x=0}^{x=1}\frac{I_{j+2}I_{jj+2}I_{ji+2,x}}{(1-x^2)}\,dx, \tag{25a}$$

$$Q(j, jj, ji) = \int_{x=0}^{x=1}\frac{xI_{j+2}I_{jj+2}I_{ji+2}}{(1-x^2)^2}\,dx, \tag{25b}$$

$i, k, m = 0, 2, 4, \ldots,$ $\quad j, l, n = 1, 3, 5, \ldots,$

$ii, ij = 0, 2, 4, \ldots,$ $\quad ji, jj = 1, 3, 5, \ldots.$

The conditions imposed on $f^{(k)}_i(r_q, t)$ and $g^{(l)}_j(r_q, t)$ are obtained in the same manner by employing (14), (16a), (16b) and are given as

$$\frac{I_q}{5r_q^2} f^{(k)}_{0,t}[r_q, t] + r_q^2 f^{(k)}_{0,r}[r_q, t] - 2r_q f^{(k)}_0[r_q, t] = 0, \tag{26}$$

$$\frac{f^{(k)}_i[r_q, t]}{2r_q^2} = \omega^{(k)}_q \delta_{k0}, \tag{27a}$$

$$g^{(l)}_j(r_q, t) = g^{(l)}_{j,r}(r_q, t) = 0, \tag{27b}$$

where $l, j = 1, 3, 5, \ldots, i, k = 0, 2, 4, \ldots,$ and $q = 1, 2.$

The corresponding initial conditions for $f_i^{(k)}$ and $g_j^{(l)}$ are obtained from (17) as

$$f_i^{(k)}(r, 0) = 0\,, \qquad g_j^{(l)}(r, 0) = 0\,, \quad \text{for all } i, j, k \text{ and } l\,. \tag{28a,b}$$

The expressions for the $k^{\text{th}}$ order approximations of the dimensionless viscous torques (18) can also be obtained in terms of the functions $f_i^{(k)}$ and $g_j^{(l)}$ by following this same procedure. This yields

$$T_q^{(k)} = \frac{1}{2}\,[r_q^2 f_{0,r}^{(k)}[r_q, t] - 2r_q f_0^{(k)}[r_q, t]]\,, \tag{29}$$

where $k = 0, 2, 4, \ldots,$ and $q = 1, 2$.

### *3.3. Solution of the zeroth-order approximation*

The mathematical model for the zeroth-order approximation, $f_0^{(0)}$, can be obtained by setting $k = i = 0$ in (23a), (24a), (26), (27a) and (28a). It consists of a homogeneous partial differential equation with nonhomogeneous boundary conditions. The form of the partial differential equation is

$$f_{0,rr}^{(0)} - \frac{2}{r^2}\, f_0^{(0)} - f_{0,t}^{(0)} = 0\,. \tag{30}$$

The solution to (30) is obtained by employing the Laplace transform method. The Laplace transform of (30) maps the dimensionless time domain ($t$) into the ($s$) domain. The general solution of the resulting ordinary differential equation is

$$\bar{f}_0^{(0)}(r, s) = r^{1/2}[AJ_{3/2}(is^{1/2}r) + BJ_{-3/2}(is^{1/2}r)]\,, \tag{31}$$

where $J_{-3/2}$ and $J_{3/2}$ are the half-order Bessel functions, and

$$\bar{f}_0^{(0)}(r, s) = \text{Laplace transform of } f_0^{(0)}(r, t)\,.$$

The constants $A$ and $B$ are determined for the various case-study problems by employing (31) in conjunction with the corresponding transformed boundary conditions. The coefficient $\bar{f}_0^{(0)}(r, s)$ has the following general form for all of the case study problems:

$$\bar{f}_0^{(0)}(r, s) = \frac{1}{s^{(0)}}\,\frac{S(r)}{Q(r)}\,. \tag{32}$$

Equation (32) can be inverted by employing the residue theorem; i.e.,

$$f_0^{(0)}(r, t) = \sum_{n=0}^{\infty} \text{Res}_n\,, \tag{33}$$

where $\text{Res}_n$ are the residues of $e^{st}\bar{f}_0^{(0)}[r, s]$. The specific forms for $S$, $Q$ and $\text{Res}_n$ for the various case-study problems can be found in [34] and are available from the author.

### 3.4. Solution of higher-order approximations

The mathematical model for the higher-order coefficients $f_i^{(k)}$ and $g_j^{(l)}$ (see (23a), (24a), (26a), (27) and (28)) is comprised of non-homogeneous partial differential equations with homogeneous boundary conditions. The solution to this model is obtained by employing the separation of variables method. In order to accomplish this, it is first necessary to determine the general solution to the homogeneous forms of the partial differential equations. These solutions can be written as

$$f_i^{(k)}(r, t) = \sum_{p=1}^{\infty} F_{ip}^{(k)}(r)\eta_{ip}^{(k)}(t) , \tag{34a}$$

$$g_j^{(l)}(r, t) = \sum_{p=1}^{\infty} G_{jp}^{(l)}(r)\eta_{jp}^{(l)}(t) , \tag{34b}$$

where $i = 0, 2, 4, \ldots$, $k = 2, 4, 6, \ldots$, $l$, $j = 1, 3, 5, \ldots$, and

$$F_{ip}^{(k)}(r) = A_{ip}^{(k)} r^{1/2} J_{(k+3/2)}(\lambda_{ip}^{(k)} r) + B_{ip}^{(k)} r^{1/2} J_{-(k+3/2)}(\lambda_{ip}^{(k)} r) , \tag{35a}$$

$$G_{jp}^{(l)}(r) = A_{jp}^{(l)} r^{1/2} J_{(l+3/2)}(\lambda_{jp}^{(l)} r) + B_{jp}^{(l)} r^{1/2} J_{-(l+3/2)}(\lambda_{jp}^{(l)} r) + C_{jp}^{(l)} r^{-(l+1)} + D_{jp}^{(l)} r^{(l+2)} ; \tag{35b}$$

$J_{\pm(l+3/2)}$ are the half-order Bessel functions, and $\lambda_{ip}^{(k)}$ are the characteristic values.

The unknown constants in (35) can be determined (relative to an arbitrary constant) for each case-study problem by employing the appropriate equations imposed on $F^{(k)}(r)$ and $G^{(l)}(r)$ (see (26), (27)). The characteristic values ($\lambda_{ip}^{(k)}$) are obtained by employing these equations and applying the condition for a nontrivial solution. It can be shown [34] that the $F_{ip}^{(k)}$ and $G_{jp}^{(l)}$ functions satisfy the general orthogonality property.

The form of the equations governing the time function $\eta_{ip}^{(k)}$ and $\eta_{jp}^{(l)}$ is obtained by substituting (34) into (23), (24) and employing this orthogonality property of the $F_{ij}^{(k)}$ and $G_{jp}^{(l)}$ functions. The resulting equations have the following general form:

$$\eta_{ip,t}^{(r)} + \lambda_{ip}^{(r)} \eta_{ip} = Z_{ip}^{(r)}(t) , \tag{36}$$

so that

$$\eta_{ip}^{(r)} = \int_0^t \mathrm{e}^{-\lambda_{ip}^{(r)}(t-\tau)} Z_{ip}^{(r)}(\tau)\, \mathrm{d}\tau . \tag{37}$$

The detailed forms of $Z_{ip}^{(r)}$, $\eta_{ip}^{(r)}$ and the equations for determining the characteristic values ($\lambda_{ip}^{(r)}$) and the constant coefficients in (35) are presented in [34] for the various case-study problems.

## 4. Results

A computer program was employed to evaluate the series for $f_i^{(k)}$, $g_j^{(l)}$, $\Omega^{(k)}$, $\Psi^{(l)}$, $\Omega$, $\Psi$, and $T_q$. The program was developed to determine the required characteristic values, orthogonality constants, integrals, etc. for each of the case-study problems. Numerical results were

obtained by running this program in double precision for various values of the dimensionless parameters. The designations for the different case studies which are discussed in this manuscript are given in Tables 1a and 1b. Future reference to the results obtained from a particular case study will be made by employing the unit code in the tables; e.g., a-IA-1 refers to case study problem (a) with $r_1/r_2 = 0.9$, $\omega_1 = 1$, $\omega_2 = 0$, and $R_2 = 10$.

### *4.1. Convergence*

The convergence of the series expansions for the variable coefficients $f_i^{(k)}$ and $g_j^{(l)}$ in (34a) and (34b) was evaluated by comparing values of these functions obtained with increasing number of terms in the series. Typical plots of the coefficients $f_i^{(k)}$ at $t = 0.005$ and $g_j^{(l)}$ at $t = 0.2$ are shown in Figs 2–4 for the impulsive torque case (case 1b). These figures show that the order of magnitude of the leading coefficients $f_i^{(i)}$ decreases significantly with increasing $i$. This was also true in the case of the coefficient $g_j^{(j)}$. Moreover, for a fixed $k$ and/or $l$, the order of magnitude remained relatively constant regardless of the values of $i$ and $j$. In general, for very small values of time ($t \leqslant 0.005$), the rate of convergence of the series for the higher-order coefficients decreases with increasing order. However, for small values of time and low values of Reynolds numbers (i.e., $R_2 \leqslant 100$), these higher-order coefficients do not contribute to the solution and, hence, can be omitted.

Figures 5–8 show typical plots of the stream function $\Psi$ vs. $r$ for the prescribed angular-velocity case, obtained for $\theta = 45°$ with increasing number of terms in the series (12a). These figures show that the number of terms required in the series increases with increasing values of Reynolds number and time. Although not shown here, this was also true for the values $T_q$, $\Omega$, and $\omega_q$. The number of required terms also increased with decreasing radius ratio ($r_1/r_2$). The series failed to converge at steady state for case-study problems a-IIIA-3 and a-IIIB-3.

*Table 1a.* Case study designations for prescribed angular velocity problem (a)

| | Case (I) $r_1/r_2 = 0.90$ | | Case (II) $r_1/r_2 = 0.50$ | | Case (III) $r_1/r_2 = 0.20$ | |
|---|---|---|---|---|---|---|
| | (A) $\omega_1 = 1$ | (B) $\omega_1 = 0$ | (A) $\omega_1 = 1$ | (B) $\omega_1 = 0$ | (A) $\omega_1 = 1$ | (B) $\omega_1 = 0$ |
| $R_2$ | $\omega_2 = 0$ | $\omega_2 = 1$ | $\omega_2 = 0$ | $\omega_2 = 1$ | $\omega_2 = 0$ | $\omega_2 = 1$ |
| 10 | a-IA-1 | a-IB-1 | a-IIA-1 | a-IIB-1 | a-IIIA-1 | a-IIIB-1 |
| 50 | a-IA-2 | a-IB-2 | a-IIA-2 | a-IIB-2 | a-IIIA-2 | a-IIIB-2 |
| 100 | a-IA-3 | a-IB-3 | a-IIA-3 | a-IIB-3 | a-IIIA-3 | a-IIIB-3 |

*Table 1b.* Case study designations for impulsive torque problem (b)

| | Case (I) $r_1/r_2 = 0.90$ $I_1 = I_2 = 4.5847$ | | Case (II) $r_1/r_2 = 0.50$ $I_1 = I_2 = 0.2426$ | | Case (III) $r_1/r_2 = 0.20$ $I_1 = I_2 = 0.00248$ | |
|---|---|---|---|---|---|---|
| | (A) $\omega_1(0) = 1$ | (B) $\omega_1 = 0$ | (A) $\omega_1(0) = 1$ | (B) $\omega_1 = 0$ | (A) $\omega_1(0) = 1$ | (B) $\omega_1 = 0$ |
| $R_2$ | $\omega_2 = 0$ | $\omega_2(0) = 1$ | $\omega_2 = 0$ | $\omega_2(0) = 1$ | $\omega_2 = 0$ | $\omega_2(0) = 1$ |
| 10 | b-IA-1 | b-IB-1 | b-IIA-1 | b-IIB-1 | b-IIIA-1 | b-IIIB-1 |
| 50 | b-IA-2 | b-IB-2 | b-IIA-2 | b-IIB-2 | b-IIIA-2 | b-IIIB-2 |
| 100 | b-IA-3 | b-IB-3 | b-IIA-3 | b-IIB-3 | b-IIIA-3 | b-IIIB-3 |

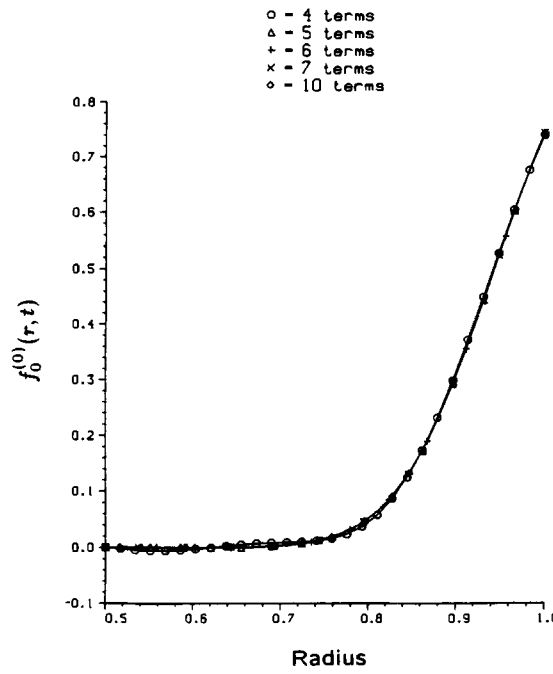


*Fig. 2.* Plot of $f_0^{(0)}(r, t)$ versus radius, case study b-IIB ($t = 0.005$).

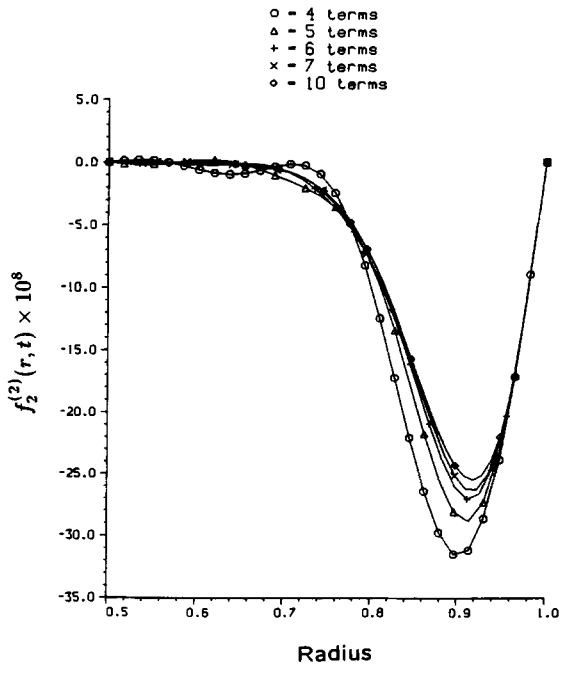


*Fig. 3.* Plot of $f_2^{(2)}(r, t)$ versus radius, case study b-IIB ($t = 0.005$).

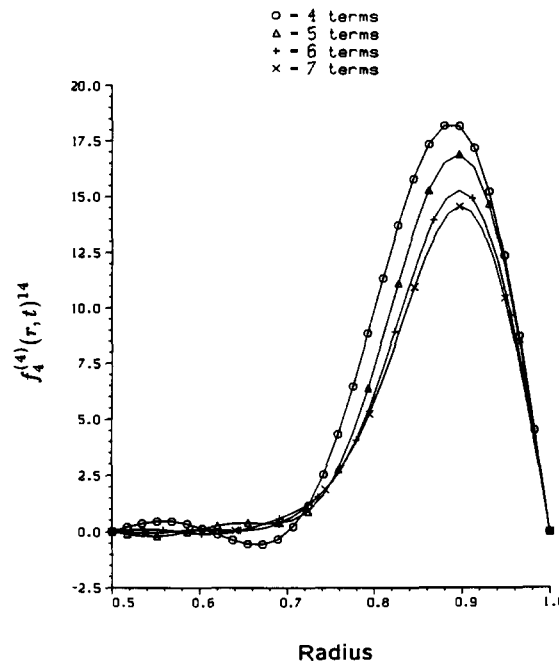


*Fig. 4.* Plot of $f_4^{(4)}(r, t)$ versus radius, case study b-IIB ($t = 0.005$).

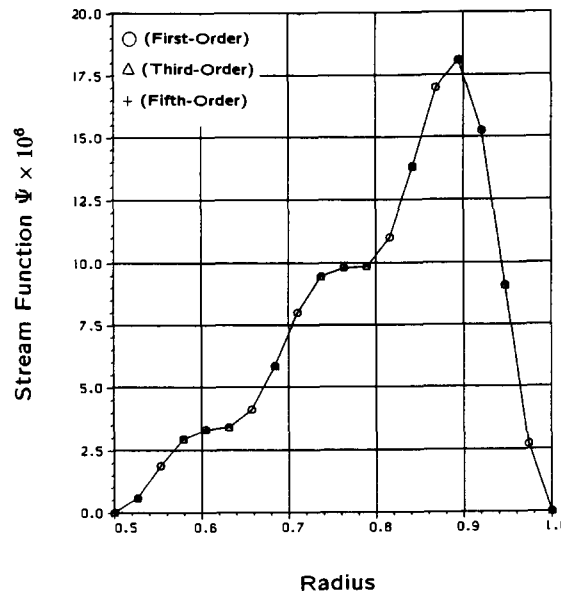


*Fig. 5.* Plot of stream function versus radius, case study a-IIB-1 ($\theta = 45°$, $t = 0.001$).

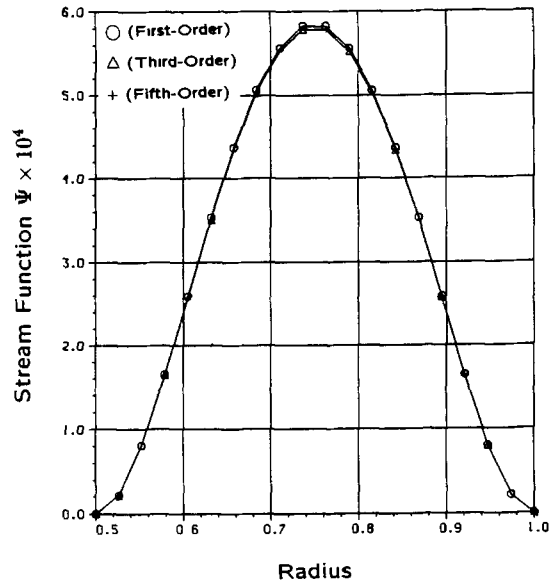


*Fig. 6.* Plot of stream function versus radius, case study a-IIB-1 ($\theta = 45°$, steady state).

### *4.2. Results for prescribed angular velocity problem*

Numerical results for $\Omega$ and $\Psi$ were obtained as a function of $x$, $r$, and $t$ for all of the case studies designated in Table 1a. Typical results for the $\Omega$ and $\Psi$ contours are shown in Figs 9–10. Contour plots for additional cases can be found in [34]. As can be seen, the contours shown in these figures are in close agreement with those obtained from Yang's [33] numerical

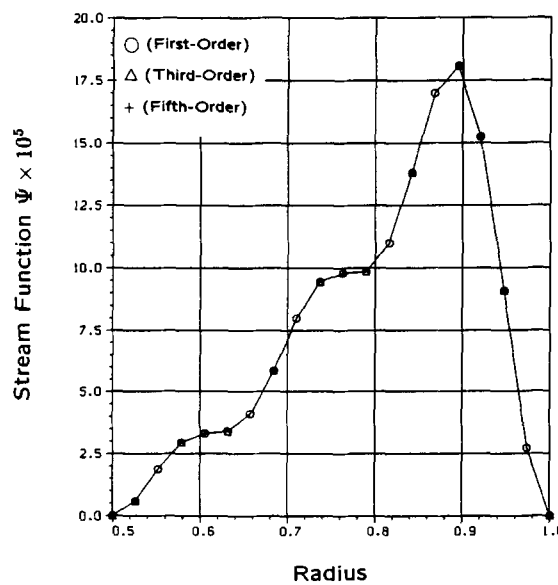


*Fig. 7.* Plot of stream function versus radius, case study a-IIB-3 ($\theta = 45°$, $t = 0.001$).

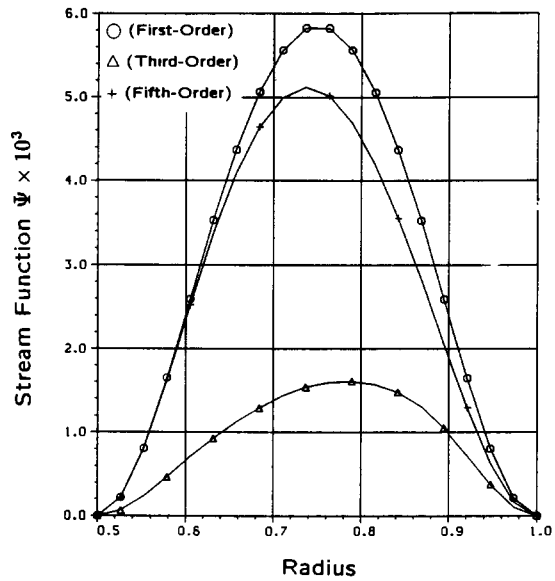


*Fig. 8.* Plot of stream function versus radius, case study a-IIB-3 ($\theta = 45°$, steady state).

solution. Although not shown here, the contours for steady flow are in good agreement with those obtained by other investigators [22, 23] for case study a-IIA-3.

Values for the viscous torques ($T_q$) for several cases are shown plotted as a function of time in Figs 11 and 12. These figures show that the viscous torques $T_1$ and $T_2$ attain the same asymptotic value at steady state. In general, the time required to attain steady state increases with decreasing radius ratio $r_1/r_2$. These figures also confirm that, for $R_2 \leqslant 100$, the higher-order terms in the series for $T_q$ do not contribute significantly when $r_1/r_2 \geqslant 0.2$ (approximately).

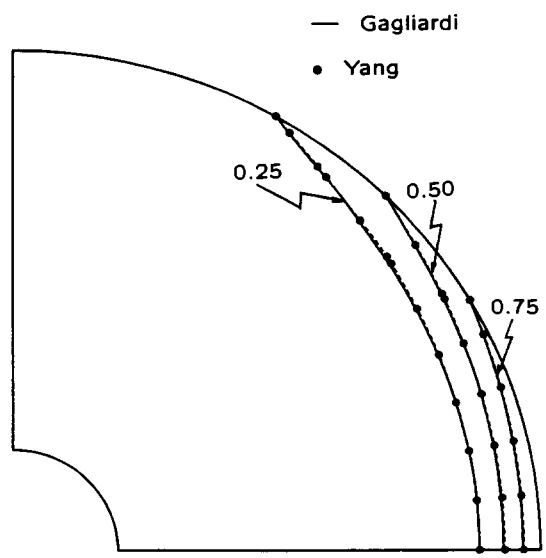


*Fig. 9.* Plot of contour lines for $\Omega$, case study a-IIIB-1 ($t = 0.005$).

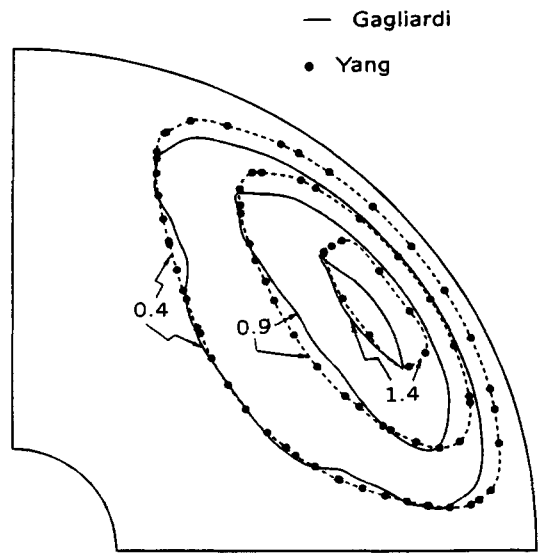


*Fig. 10.* Plot of contours lines for $10^4\,\Psi$, case study a-IIIB-1 ($t = 0.005$).

The results for the steady state viscous torques ($T_q$) are plotted as a function of the radius ratio $r_2/r_1$ for $R_1 = 15$ and 45 in Figs 13–14. The results in these figures are shown compared to: (a) the limiting values ($r_2/r_1 \to \infty$) obtained from Dennis, Singh, and Ingham [31], (b) values predicted by the Couette-flow theory ($r_2/r_1 \to 1$), and (c) values obtained by Yang's [33] numerical solution. The comparisons shown in these figures indicate that flow in an annulus with $r_2/r_1 \geq 4$ (approximately) furnishes a reasonable representation of the flow around a sphere rotating in an infinite medium for cases where $R_1 \leq 45$. These figures also show that the results from this investigation approach those predicted by the Couette theory

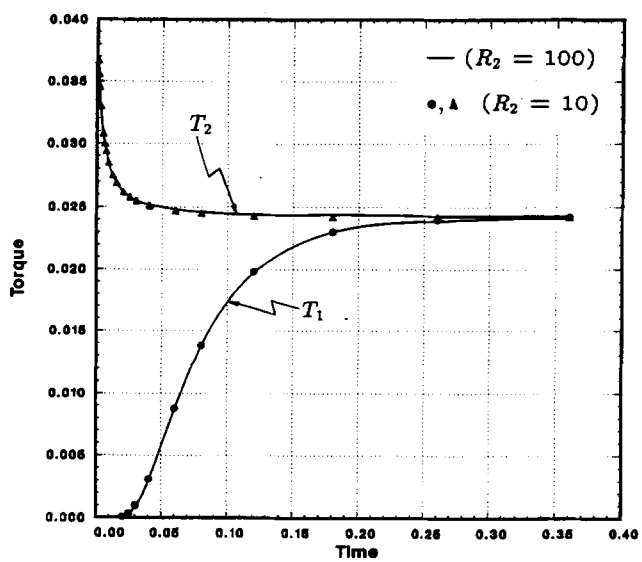


*Fig. 11.* Plot of viscous torque vs. time, case study a-IIIA.

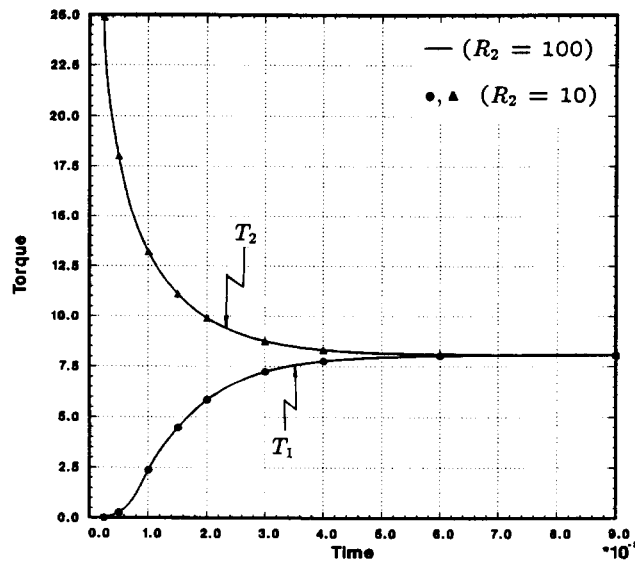


*Fig. 12.* Plot of viscous torque vs. time, case study a-IA.

as $r_2/r_1 \to 1$, and are in good agreement with those obtained from Yang's [33] numerical solution. Moreover, these figures indicate that, for this range of $R_1$, the torques $T_q$ are independent of $R_1$ for $r_2/r_1 \leq 1.7$ (approximately).

A comparison of the steady-state torques ($T_q$) obtained by several investigators is shown in Table 2 for case studies a-IIA-3 and a-IIB-3. It can be seen from this table that the results of these investigations agree favorably.

### *4.3. Resuts for impulsive torque problem*

Typical results for the $\Omega$ and $\Psi$ contours for the impulsive torque problem are shown in Figs 15–16. Contour plots for additional cases can be found in [34]. As can be seen, the contours

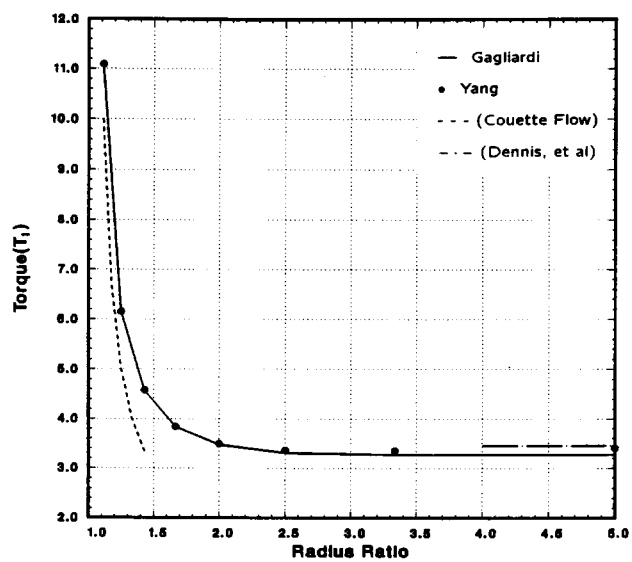


*Fig. 13.* Plot of viscous torque ($T_1$) vs. radius ratio, case study a-A ($R_1 = 15$, steady state).

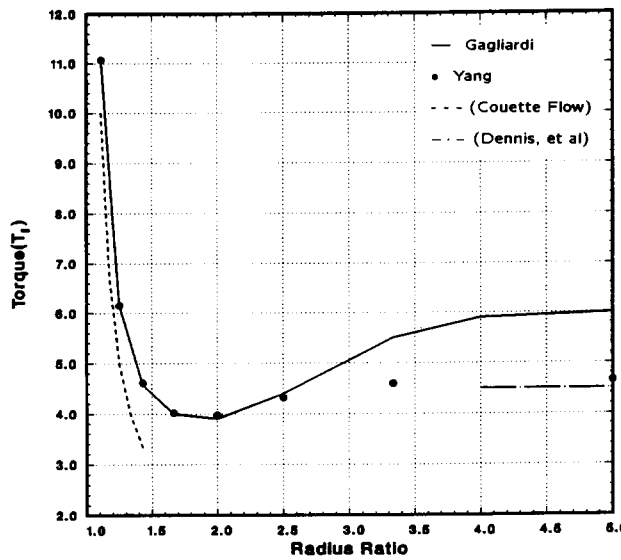


*Fig. 14.* Plot of viscous torque ($T_1$) vs. radius ratio, case study a-A ($R_1 = 45$, steady state).

*Table 2.* Comparison of results for steady-state viscous torques

| Investigator | Case study a-IIB-3 | Case study a-IIA-3 |
|---|---|---|
| Gagliardi et al. | 0.486 | 0.445 |
| Yang et al. [33] | 0.499 | 0.446 |
| Dennis and Singh [7] | 0.500 | 0.446 |
| Dennis and Quartapelle [24] | 0.517 | 0.445 |
| Munson and Joseph [5] | 0.497 | 0.441 |

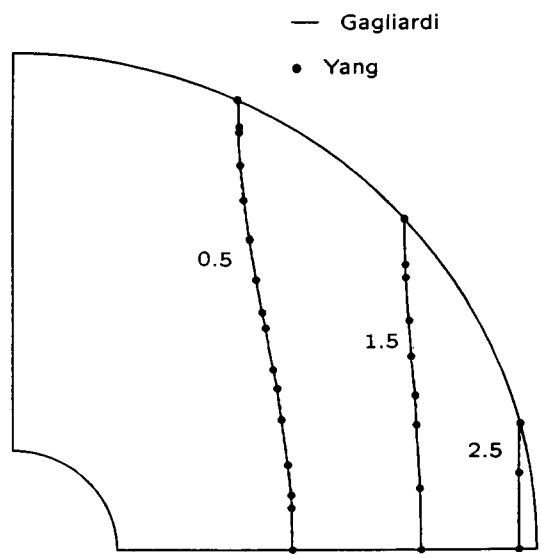


*Fig. 15.* Plot of contour lines for $10^3\ \Omega$, case study b-IIIB-2 ($t = 0.05$).

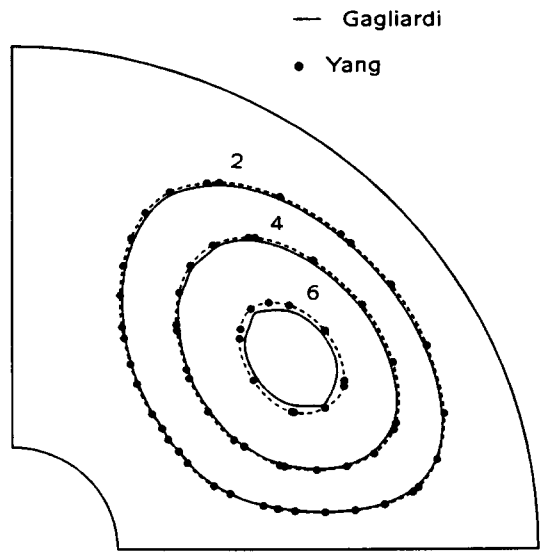


*Fig. 16.* Plot of contour lines for $10^8\ \Psi$, case study b-IIIB-2 ($t = 0.05$).

shown in these figures are in good agreement with those plotted from Yang's [33] results. In general, the results for the impulsive torque problem from this investigation were in good agreement with those obtained by Yang [33] for all cases where $R_q \leqslant 100$ and $r_2/r_1 \leqslant 2$. Profiles at $\theta = 45°$ of $\Omega$ and $\Psi$ obtained from this investigation are also shown plotted in Figs 17–18 as a function of time for various values of the radius $r$. These figures show the build-up and asymptotic decay of the motion of the fluid contained in the spherical annulus.

Typical magnitudes of the viscous torques ($T_q$) are presented as a function of time in Figs 19–20. These figures show that the magnitude of the viscous torque on the stationary sphere

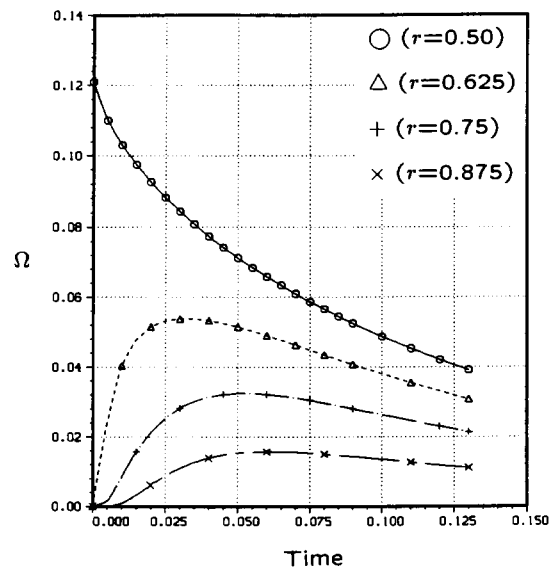


*Fig. 17.* Plot of $\Omega$ vs. time, case study b-IIA-1 ($\theta = 45°$).

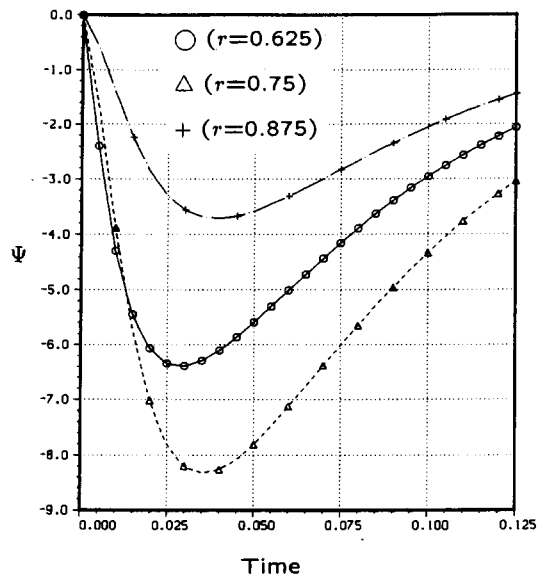


*Fig. 18.* Plot of $\Psi$ vs. time, case study b-IIA-1 ($\theta = 45°$).

increases with time from zero to a maximum value and then decreases asymptotically back to zero. Figure 20 shows that, for the narrow-gap cases ($r_1/r_2 \geq 0.9$), the viscous torque on the stationary sphere builds up very rapidly and attains a value equal in magnitude to that acting on the rotating sphere. This can be attributed to the dominance of the viscous effect in this case. The figures also show good agreement between the results of this investigation and those obtained from Yang [33].

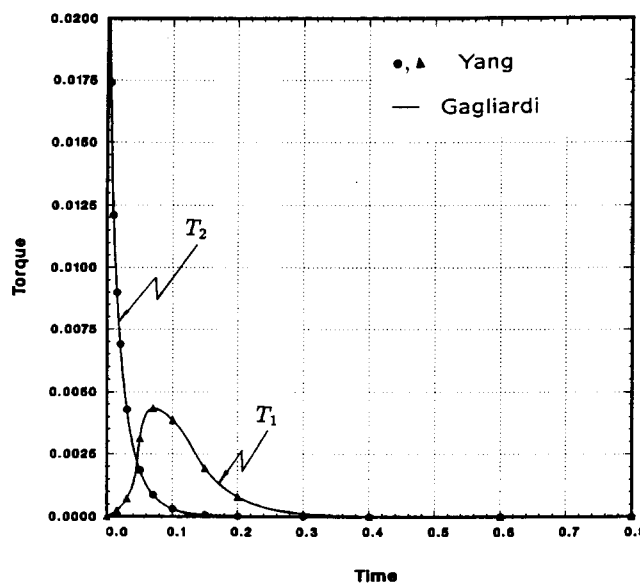


*Fig. 19.* Plot of viscous torque vs. time, case study b-IB-1.

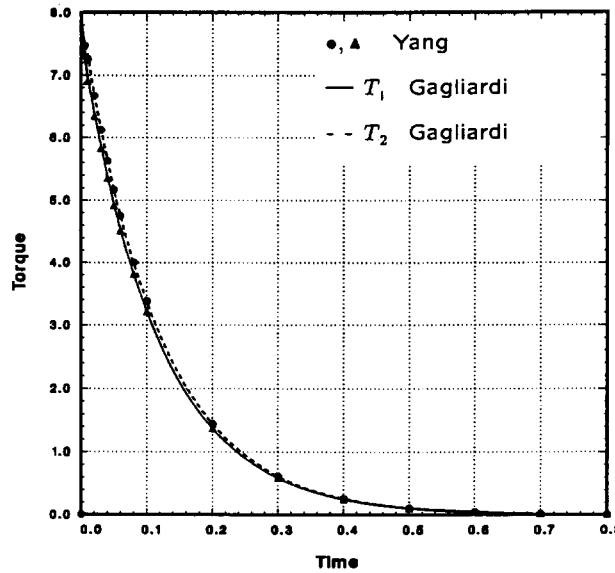


*Fig. 20.* Plot of viscous torque vs. time, case study b-IIIA-3.

Plots of the angular velocity ($\omega_2$) vs. time are shown in Figs 21 and 22. These plots show that the value of the dimensionless angular velocity decays asymptotically from the initial value to zero. In general, the rate of decay increases with increasing radius ratio ($r_1/r_2$) and decreasing inertia ratio ($I_1$). The figures also show that the results from this investigation are in good agreement with those obtained by Yang's [33] numerical solution.

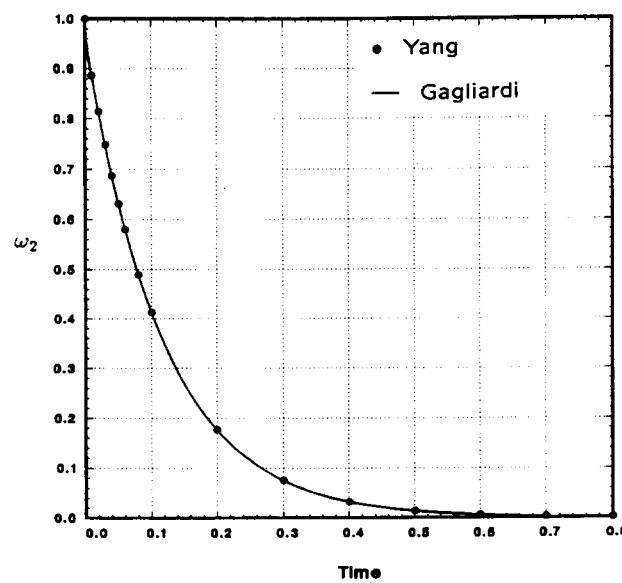


*Fig. 21.* Plot of $\omega_2$ vs. time, case study b-IB-3.

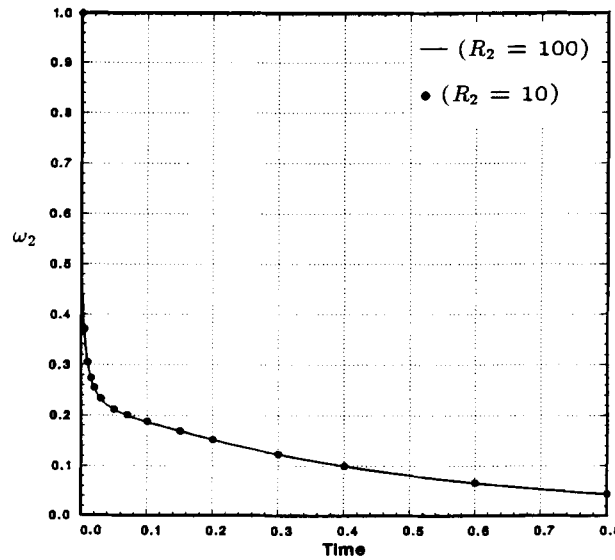


*Fig. 22.* Plot of $\omega_2$ vs. time, case studies b-IIB-1 & b-IIB-3.

## 5. Conclusion

The primary purpose of the research reported in this paper was to study the use of the perturbation method with series truncation, by use of orthogonal Gegenbauer polynomials, to analyze the transient motion of a fluid in an annulus between two concentric spheres which are started suddenly due to the action of prescribed torques. The comparison of the results obtained from this and other investigations, in particular Yang [33], indicates that this method can be used satisfactorily for small Reynolds numbers ($R_2 \leq 100$) and radius ratios $r_1/r_2 \geq 0.2$. The method has the advantage that, for small Reynolds numbers, only few terms are required in the series expansions for $\Omega$ and $\Psi$ and, hence, it is practical for obtaining the solution in closed form.

## References

1. I. Proudman, The almost-rigid rotation of viscous fluid between concentric spheres, *Journal of Fluid Mechanics* 1 (1956) 505–516.
2. K. Stewartson, On almost rigid rotations, Part 2, *Journal of Fluid Mechanics* 26 (1965) 131–144.
3. G.F. Carrier, Some effects of stratification and geometry in rotating fluids, *Journal of Mechanics* 23 (1965) 145–172.
4. W.C. Haberman, Secondary flow about a sphere rotating in a viscous liquid inside a coaxially rotating spherical container, *Physics of Fluids* 5 (1962) 625–626.
5. B.R. Munson and D.D. Joseph, Viscous incompressible flow between concentric rotating spheres, Part 1: Basic flow, *Journal of Fluid Mechanics* 49 (1971) 289–303.
6. J. Pedlosky, Axially symmetric motion of a stratified rotating fluid in spherical annulus of a narrow gap, *Journal of Fluid Mechanics* 36 (1969) 401–415.
7. S.C.R. Dennis and S.N. Singh, Calculation of the flow between two rotating spheres by the method of series truncation, *Journal of Computational Physics* 28 (1978) 297–314.

8. D. Greenspan, Numerical studies of steady, viscous, incompressible flow between two rotating spheres, *Computers and Fluids* 3 (1975) 68–82.
9. D. Schultz and D. Greenspan, Improved solution of steady, viscous, incompressible flow between two rotating spheres, *Computers and Fluids* 7 (1979) 157–163.
10. G. Schrauf, Branching of Navier–Stokes equations in a spherical gap, Eighth international conference on numerical methods in fluid dynamics (Edited by E. Krause), *Lecture Notes in Physics* 170 (1982) 474–480.
11. P. Bar-Yoseph, J.J. Blech and A. Solan, Finite element solution of the Navier–Stokes equations in rotating flow, *International Journal for Numerical Methods in Engineering* 17 (1981) 1123–1146.
12. M.P. Sorokin, G.N. Khlebutin and G.F. Shaidurov, Study of the motion of a liquid between two rotating spherical surfaces, *Journal of Applied Mechanics and Technical Physics* 7 (1966) 73–74.
13. G.N. Khlebutin, Stability of fluid motion between a rotating and a stationary concentric sphere, *Fluid Dynamics* 3 (1968) 31–32.
14. J. Zierep and O. Sawatzki, Three-dimensional instabilities and vortices between two rotating spheres, *Eighth Symposium on Naval Hydrodynamics* (1970) 275–288.
15. B.R. Munson and M. Menguturk, Viscous incompressible flow between concentric rotating spheres, Part 3: Linear stability and experiments, *Journal of Fluid Mechanics* 69 (1975) 705–719.
16. M. Wimmer, Experiments on a viscous flow between concentric rotating spheres, *Journal of Fluid Mechanics* 78 (1976) 317–335.
17. M. Wimer, Experiments on the stability of viscous flow between two concentric rotating spheres, *Journal of Fluid Mechanics* 103 (1981) 117–131.
18. K. Nakabayashi, Frictional moment of flow between two concentric spheres, one of which rotates, *Journal of Fluid Engineering* 100 (1978) 97–106.
19. A.M. Waked and B.R. Munson, Torque characteristics for spherical annulus flow, *Journal of Fluid Engineering* 101 (1979) 284–286.
20. A.M. Waked and B.R. Munson, Laminar-turbulent flow in a spherical annulus, *Journal of Fluid Engineering* 100 (1978) 281–286.
21. B.R. Munson and R.W. Douglas, Viscous flow in oscillatory spherical annuli, *Phys. Fluids* 22 (1979) 205–208.
22. C.E. Pearson, A numerical study of the time dependent viscous flow between two rotating spheres, *Journal of Fluid Mechanics* 28 (1967) 323–336.
23. C.E. Pearson, A numerical method for incompressible viscous flow problems in a spherical geometry, in: *Studies in numerical analysis I*, SIAM, Philadelphia, Pennsylvania (1968) 65–78.
24. S.C.R. Dennis and L. Quartapelle, Finite difference solution to the flow between two rotating spheres, *Computers and Fluids* 12 (1984) 79–92.
25. E. Krause and F. Bartels, Finite-difference solution of the Navier–Stokes equations for axially symmetric flows in spherical gaps, *Lecture Notes in Mathematics* 771 (1979) 313–322.
26. F. Bartels, Taylor vortices between two concentric rotating spheres, *Journal of Fluid Mechanics* 119 (1982) 1–25.
27. C.R. Illingworth, Boundary layer growth on a spinning body, *The Philosophical Magazine* 45 (1954) 1–8.
28. E.R. Benton, Laminar boundary layer on an impulsively started rotating sphere, *Journal of Fluid Mechanics* 23 (1965) 611–623.
29. K.E. Barrett, On the impulsively started rotating sphere, *Journal of Fluid Mechanics* 27 (1967) 779–788.
30. S.C.R. Dennis and D.B. Ingham, Laminary boundary layer on an impulsively started rotating sphere, *Physics of Fluids* 22 (1979) 1–9.
31. S.C.R. Dennis, S.N. Singh and D.B. Ingham, The steady flow due to a rotating sphere at low and moderate Reynolds Numbers, *Journal of Fluid Mechanics* 101 (1980) 257–279.
32. H. Takagi, Viscous flow induced by slow rotation of a sphere, *Journal of the Physical Society of Japan* 42 (1977) 319–325.
33. Yang Jen-Kang, *Numerical Studies of Axially Symmetric Motion of an Incompressible Viscous Fluid Between Two Concentric Rotating Spheres*, Ph.D. dissertation, Marquette University (1987).
34. J.C. Gagliardi, *Analytic Studies of Axially Symmetric Motion of an Incompressible Viscous Fluid Between Two Concentric Rotating Spheres*, Ph.D. Dissertation, Marquette University (1987).